Distributed Control for Laneless and Directionless Movement of Connected and Automated Vehicles

Kimia Chavoshi

Anastasios Kouvelas

Conference paper STRC 2021

Distributed Control for Laneless and Directionless Movement of Connected and Automated Vehicles

Kimia Chavoshi
IVT
ETH Zurich
kimia.chavosi@ivt.baug.ethz.ch

Anastasios Kouvelas
IVT
ETH Zurich
anastasios.kouvelas@ivt.baug.ethz.ch

Abstract

Laneless and directionless movement is a novel traffic characteristic of trajectory behavior for Connected and Automated Vehicles (CAVs) in highway networks. Applying this concept can exploit the highway's maximum potential capacity, especially under unevenly distributed directional demand. Nevertheless, the elimination of the conventional notion of vehicles' movements on the separated domains of lanes and directions, can consequently increase the chaotic driving behavior and collision risks (and thus jeopardize safety). Hence, the paper is focused on trajectory planning for CAVs in such a futuristic environment with the twofold objective of (i) providing and guaranteeing safety, while (ii) improving the traffic performance. To this end, we propose an algorithm for CAVs to distinguish potential conflicting vehicles from their own direction and/or opposing traffic stream (the so-called threats throughout this document) in an early (timely) stage. Afterwards, the threat vehicles are clustered as threat groups. As the next step, a decentralized NonLinear Model Predictive Control (NLMPC) framework is developed to regulate the movement of vehicles within each single threat cluster; in that sense, this is a distributed controller applied in each cluster separately. The control method is designed in a manner to fulfill the above mentioned twofold objective, combining traffic safety and efficiency. Finally, the performance of the proposed method is investigated and assessed through a microscopic simulation study. The results are promising and confirm the effectiveness of the proposed method for highway networks.

Keywords

Laneless traffic, Directionless traffic, Connected and Automated vehicles, Distributed Control, Model Predictive Control, Highway traffic networks.

1 Introduction

The advent of fully Connected and Autonomous Vehicles (CAVs) will make a revolutionary change in the existing transportation reality Hancock *et al.* (2019); Elliott *et al.* (2019). The deployment of CAVs can improve the performance of transportation systems in teRMSE of safety, capacity usage, congestion, etc. (see Kim and Kumar (2014); Talebpour *et al.* (2017)). Moreover, the recent technological developments enable us to provide novel approaches and solutions for the various transportation problems. For instance, thanks to the CAV technology, different researchers (see e.g. Xu *et al.* (2018); He *et al.* (2018); Makarem and Gillet (2013); Mitrovic *et al.* (2019); Chavoshi *et al.* (2021)) have proposed the concept of lightless intersection to increase the serving capacity of urban arterials. Along the way, the specific characteristics of CAVs on highway networks can be utilised to enhance the performance of traffic systems.

For instance, although most of the traffic control methods are developed for lane-based traffic Zheng (2014); Talebpour *et al.* (2015); Asaithambi *et al.* (2016); Wang *et al.* (2019), new studies have recently proposed the laneless concept in order to increase the capacity of the freeway Papageorgiou *et al.* (2021); Mulla *et al.* (2019); Chavan *et al.* (2016); Troullinos *et al.* (2021a). Laneless traffic can be described as the nonexistence of predefined lanes for the vehicles' movement. Therefore, the vehicles do not have to adhere to any lane discipline and are free to choose an arbitrary lateral position for their movement in the highway. This is similar to the behavior of motorcycles (swerving or oblique following of the leading vehicle) during the traffic congestion Nguyen *et al.* (2014). Through this method, we can serve more vehicles on the highway cross section. So far, the control methods that have been proposed for CAVs movement are designed based on the separation for longitudinal and lateral movements that are inapplicable for the laneless environment Gueriau *et al.* (2016); Zhou *et al.* (2017); Zhu and Zhang (2018). Consequently, the current research is focusing on designing an interactive control for CAVs in the laneless environment. For example, the study in Papageorgiou *et al.* (2021) introduced vehicle nudging to model the force of a vehicle to the vehicles that are in front. The work Chavan *et al.* (2016) proposed the influence graph in both lateral and longitudinal dimensions to model the interaction between CAVs. Finally, Troullinos *et al.* (2021b) utilized the max-plus algorithm with 'artificial potential fields' to design a coordinated control method for CAVs in lane-free environment.

Although the laneless traffic can increase the capacity usage of the highway, it cannot reach the optimal point when the demand flows on different directions (left to right or light to left) of the highway are imbalanced. Note, that Chavoshi and Kouvelas (2020)

has addressed this situation and proposed the laneless and directionless approach to maximize the capacity usage in both directions of a highway. The directionless concept is introduced as eliminating the conventional dedicated space for different directional movements in highways. The main idea is depicted visually in Figure 4, where CAVs with different directions are able to use the whole width of the highway. Although the studies have proven that the directionless method is capable of improving the performance of the highway from macroscopic perspective Malekzadeh *et al.* (2021), it simultaneously increases the complexity level of CAVs movement control. In fact, CAVs in the laneless and directionless environment have higher risk of collisions. In this paper, we focus on designing a proper control method that can deal with optimizing the trajectories of CAVs in a laneless and directionless environment. The proposed controller is designed such as to guarantee the safety in the microscopic level and decrease the total travel time in the network level, as it causes the CAVs to move at their desired velocities.

The rest of the paper is organized as follows: In the next section, we present the problem statement and describe the dynamic equations that we utilize for the modeling of individual CAV's movement. Next, we describe the methodology, where the concepts of neighbor, threat, and threat group are introduced; afterwards, according to these concepts, we design the control strategy. In the following section, we provide the simulation results to verify the methodology and describe its pipeline. Finally, the last section presents the next steps and future directions of this research.

2 Problem Formulation

As we already mentioned, the laneless and directionless traffic concept is proposed to maximize the throughput of the highway infrastructures for different demand patterns. This novel traffic concept is established on the CAVs ability to move freely with in the highway width. The predefined microscopic traffic models for CAVs, car following and lane changing, are designed to formulate the CAVs' movement for the conventional infrastructure with separated lanes and directions. Consequently, the previous microscopic methods are not applicable to this new traffic environment. In this study, we present a new method for the microscopic traffic movement of CAVs in laneless and directionless environment. The proposed method enables the CAVs to plan their optimal trajectories while guaranteeing the safety and collision avoidance.
In the following, we list the assumptions that are considered in this paper.

- The traffic flow contains merely CAVs (CAV penetration rate of 100%).
- CAVs are homogeneous is shape and specifications. They are considered to have square shape with the uniform width. In addition, they have the same driving specifications (uniform acceleration, deceleration, and speed range).
- Every CAV can communicate with other CAVs within a radius around them, i.e., it is able to access information such as current speed, position, and heading angle.

2.1 Kinematics model for CAVs

In this section, we model the individual CAV movement according to the basic kinematics model. In order to avoid the complexity in this level, the details related to the vehicle dynamics (steering angle, yaw rate, lateral and longitudinal forces of tiers, etc.) are excluded, and we focus on a much simpler model that can capture all the characteristics from a traffic flow theory viewpoint. Figure 1 shows the coordinate system of the CAV movement, where x and y are, respectively, the longitudinal and lateral axes, that (without loss of generality) are, respectively, parallel and perpendicular to the highway boundaries. The velocity is denoted by v, and θ is the heading angle. One can derive the longitudinal and lateral movement of a CAV by projecting v with respect to θ on x and y axes. Thereby, for CAV i, the movement dynamics model can be defined as follows:

$$\begin{cases} x_i(k+1) = x_i(k) + Tv_i(k)\cos(\theta_i(k)) \\ y_i(k+1) = y_i(k) + Tv_i(k)\sin(\theta_i(k)) \\ v_i(k+1) = v_i(k) + Ta_i(k) \end{cases}, \tag{1}$$

where $k = 0, 1, \ldots$ is the discrete time-step and T (s) denotes the sampling time. The variables $x_i(k)$ (m), $y_i(k)$ (m) and $v_i(k)$ (m/s) denote the states of the system, while the acceleration $a_i(k)$ (m/s^2) and the steering angle $\theta_i(k)$ (rad) are the control input signals.

Figure 1: The diagram of the CAV movement.

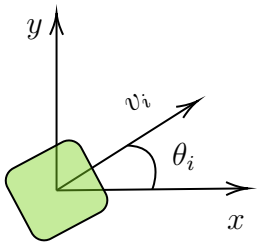

3 Methodology

In this study, we assumed the CAVs are equipped with the V2V (vehicle to vehicle) and V2I (vehicle to infrastructure) capabilities. Thus every CAV has access to its neighbors' information. These information provide the CAV with a crucial perception for the space in its vicinity and enable it to predict the potential collisions and detect the "threating" vehicles (i.e., vehicles that can constitute possible collisions in the near future). Furthermore, the threating vehicle may also be threatened by another vehicle; as a result, we can construct a chain of the vehicles that their movements depend on each other and refer to it as a threat group. Thereby, the idea is to develop a decentralized MPC-based control methodology for the movement of all CAVs that belong to the same threat group. We assume that the traffic system is discrete-time, in the sense that any CAV can take an action at discrete time steps. We perform the control of any CAV by providing an appropriate control signals $a_i(k)$ and $\theta_i(k)$. Finally, we assume that the CAVs are restriceted to move within the boundaries of the highway.

3.1 Neighbors and threats

For each CAV, we define the neighborhood as a circle centered in the center of geometry of the CAV. We name the radius of this circle as the communication radius (Figure 2). The communication radius must be long enough as to cover all the possible threats; moreover, the CAV must have enough time to react and avoid the collision with the threats within the time they are detected in the neighborhood border. In order to formulate this communication radius, we extend the concept of safe distance in the classical car-following model. Essentially, in the most of car-following models, the safe distance contains two common terms. One term expresses the impact of driver's reaction time. Besides that, the safe distance includes another term that describes the required crucial distance as a consequence of the relative speed between the leader and the follower. For CAVs, the first term is a technical specification and can be interpreted as the distance with regards to communication time delays T_{cd}. Moreover, similar to the car-following model, the second term, namely vital gap (VG), is also required for CAVs. Vital gap expresses the longest gap which is required in the worst case to avoid collision. The worst case in the directionless environment for CAV i occurs when a neighbor is heading towards it with the maximum speed $v_{\max}$. Thus, for CAV i, the vital gap is the required distance to another conflicting CAV in the worst case scenario, so as to make the relative speed equal to zero:

$$\mathrm{VG} = \frac{(v_i + v_{\max})^2}{4a_{\mathrm{dec}}}. \tag{2}$$

In equation (2), v_i is the velocity of the CAV i, and a_{dec} is the maximum deceleration. Due to the fact that in our methodology, both conflicting CAVs can take action, the maximum relative acceleration (deceleration) is $2a_{\mathrm{dec}}$. Therefore, the communication radius R_i is given by

$$R_i = T_{\mathrm{cd}} v_i + \frac{(v_i + v_{\max})^2}{4a_{\mathrm{dec}}}. \tag{3}$$

According to the above mentioned equation, the faster a CAV is moving, the larger the neighborhood it has. In Figure 2, the yellow circle with the radius R, centered on the green CAV, demonstrates the neighborhood for this specific CAV. As mentioned above, this yellow circle represents also the maximum communication range, so the green CAV does not need to have any communication with the vehicles that are outside the neighborhood (blue vehicles in Figure 2). For CAV i, the neighbor set $\mathcal{N}_i$ is defined as:

$$\mathcal{N}_i = \{jD_{i,j} \leq R_i\} \tag{4}$$

$$D_{i,j} = \sqrt{(x_i - x_j)^2 + (y_i - y_j)^2}\ , \tag{5}$$

Figure 2: Graphical definition of the neighborhood. The yellow circle depicts the neighborhood for the green CAV, and the blue CAVs indicate vehicles that are outside the communication region. The rest of CAVs are the neighbors, whereas, only the red one constitutes a threat.

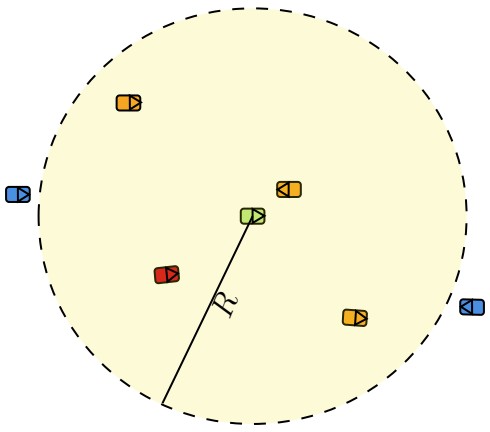

where $D_{i,j}$ denotes the distance between CAVs i and j. In Figure 2, the vehicles that are inside the yellow circle are defined as the green CAV's neighbors. The neighbors with a potential collision risk are the threats (for instance the red vehicle in Figure 2) and the CAV only needs to react to the threats. Therefore, as the next step, it is essential to distinguish the threats from the neighbors. The threat relationships should be investigated based on collision risk factors, relative distance, and movement direction. We utilize a similar concept as vital gap to determine the bound for relative distance in a threat relationship. As we mentioned, the vital gap provides the required distance of CAV i from another conflicting CAV in the worst case scenario. Hence, to customize this vital gap for the potential threat, CAV k, we replace $v_i + v_{\max}$ in equation (2) with the magnitude of the relative speed $S_{k,i}$ of vehicles and k and i, respectively.

In order to determine the direction with the risk of collision, we assume that every CAV is surrounded by a safe margin that describes the area where no other vehicles' centroid should enter at any time. In Figure 3 the yellow circle with the radius of r_{m} represents the safe margin for the green CAV. The radius of the safe margin is defined as $r_{\mathrm{m}} = \sqrt{2}w$, where w is the width of CAV. This formula represents the longest distance between two CAVs' centriods when they collide; which is equal to the diagonal of a CAV. In order to define the threat candidates, we denote the maximum area by connecting the CAV's centeriod to the other vehicle's safe margin (tangent lines to the circle) and creates the risk spectrum. A neighbor is a threat if its relative distance is smaller than the customized vital gap and its relative speed vector is inside the risk spectrum (see Figure 3). For CAV i, the threat set $\mathcal{T}_i$ which is a subset of $\mathcal{N}_i$ is defined as follows:

$$\vec{S}_{k,i} = \vec{v}_k - \vec{v}_i \tag{6}$$

$$\mathcal{T}_i = \left\{ kk \in \mathcal{N}_i,\ D_{k,i} \leq \frac{(S_{k,i})^2}{4a_{\mathrm{dec}}},\ \angle\vec{D}_{k,i} - \arcsin\frac{r_m}{D_{k,i}} \leq \angle\vec{S}_{k,i} \leq \angle\vec{D}_{k,i} + \arcsin\frac{r_m}{D_{k,i}} \right\}, \tag{7}$$

where $\vec{v}_k$ is the velocity vector with a magnitude v_k and an angle θ_k; $\vec{S}_{k,i}$ denotes the vector of the relative speed between CAVs k and i, respectively.

Note that the threat relationship is a reciprocal concept. Two CAVs that have threat relationship must take actions to avoid collision. However, each of them may also be threaten by other vehicles that should be considered to make a correct action. As a result, we define a threat group as a chain of CAVs that are related to each other due to the

threat relationship. Figure 4 demonstrates an example of our study environment, where the pink areas represent different threat clusters or threat groups.

3.2 Control Approach

As described in the previous section, we cluster all the CAVs that can probably collide into the threat groups. A CAV belongs to the threat group $\mathcal{G}_i$ if it threatens at least one of the members of $\mathcal{G}_i$. The objective of this study is to control the movement of each CAV in a decentralized manner, to avoid the collision, and, besides that, decrease the total travel time by maintaining the optimal trajectory in each individual's movement. Given the fact that threat relations are time-varying, it is crucial to have a future horizon-based controller. Model Predictive Controller (MPC) is one appropriate horizon-based controller. In principle, MPCs have the advantage of considering the impact of the predicted future behavior of the system on the current control signal derivation. This feature of MPC enables us to design the CAV's movement such that it avoids the neighboring threats, and meanwhile, it does not create undesirable threats for other neighbors. To this end, for every threat group $\mathcal{G}_i$, we define the MPC problem formulation as follows:

$$\min_{a_j,\theta_j} \left(\sum_{k=1}^{p} \left(\sum_{j\in\mathcal{G}_i} \left(\alpha_j(\theta_j(k) - \theta_j^{\mathrm{d}})^2 + \beta_j(v_j(k) - v_j^{\mathrm{d}})^2 \right) \right) + \sum_{j=1}^{N_T} \gamma_j(\epsilon_j)^2 \right) \tag{8}$$

Figure 3: Threat detection. The yellow rectangle represents the safety margin for the green CAV and the blue area demonstrate the risk spectrum.

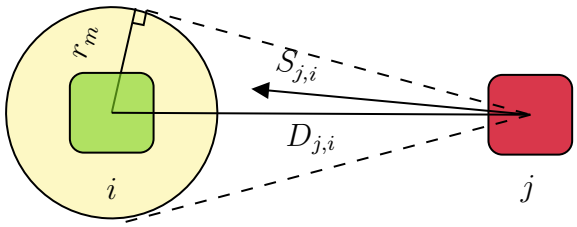

Figure 4: An example of the laneless and directionless movement on highway. The pink areas determine the threat clusters.

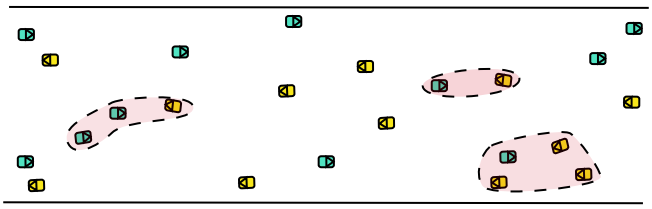

subject to state space model (1) and:

$$\left|\Delta y_i\right| \geq \alpha(\frac{R - D_{j,l}}{D_{j,l}}) + \epsilon_i, \quad \forall i \in \left[1,\ N_T\right] \tag{9}$$

$$a_{\min} \leq a_j(k) \leq a_{\max} \tag{10}$$

$$\left|\Delta a_j(k)\right| \leq \delta_a \tag{11}$$

$$\left|\theta_j(k) - \theta_d\right| \leq \frac{\pi}{3} \tag{12}$$

$$\left|\Delta \theta_j(k)\right| \leq \delta_\theta \tag{13}$$

$$0 \leq v_j(k) \leq v_{\max} \tag{14}$$

$$y_{\min} \leq y_j(k) \leq y_{\max} \tag{15}$$

where j denotes the index of the CAVs that belong to $\mathcal{G}_i$; and k indicates the step time within the prediction horizon p. Note that the control horizon is considered to be equal with the prediction horizon. The objective function is shown in equation (8), and it consists of three terms. The first term is designed to minimize the deviation of the angle from desired point θ_k^{d} (which is defined by the destination, i.e., for the left to the right movement is 0 and for the right to the left movement is π). The second term expresses the convergence of speed v_k to the desired speed v_k^{d}. The last term is designed concerning the goal of avoiding collision between threats. Based on equation (9), ϵ_i is the deviation from the designed trajectory. Every threat group $\mathcal{G}_i$ contains N_T number of threat pairs.

Assume threat pair number i consists of CAVs j and k, Δy_i denotes the lateral distance

between the centroids of CAVs k and j, respectively. The desired value for the lateral distance of threat pair i, is calculated with $\alpha\big((R-D_{j,k})/D_{j,k}\big)$; where R is the communication radius. This equation expresses the trajectory for the lateral distance of a threat pair. According to (9), by decreasing the relative distance $D_{j,k}$; the desired lateral distance is gradually increasing with a linear trend from zero to α. When the relative distance of the threat pair $D_{j,k}$ is zero, Δy_i is larger than α. Note the α is equal with $w+\delta$, where δ is the minimum lateral distance between CAVs. ϵ_i only penalises the cases where Δy_i is smaller than the corresponding desired trajectory. The variables α_j and β_j and γ_j are the weights for the different terms of objective function. The vehicles' movement is confined with the physical constraints (10)–(15), where (10) represents the bounds for acceleration; (11) shows the limitation on acceleration differential; (12) is defined to bound the vehicles' heading angle; (13) limits the derivative of the heading angle; constraint (14) bounds the speed magnitude; and finally, constraint (15) limits the lateral position of the vehicles inside the highway.

4 Microscopic simulation results

In this section, we design a case study to investigate the applicability and efficiency of the methodology and its pipeline. We report the results of this experiment as a proof of concept. The case study composed of two platoons of CAVs in a highway moving on the same lateral position towards each other. Figure 5 demonstrates twelve different time snapshots of the simulation for this experiment. Each square depicts one CAV, and its arrow represents the vehicles' speed vector. Furthermore, the CAVs associated to the same threat cluster are distinguished with black borders. The initial setup is shown in Figure 5 for the time step $k=90$. The first platoon (indicated with red vehicles) composed of 12 CAVs in three columns and four rows, moving toward right ($\theta=0$); with the initial lateral distance and longitudinal distance of 2m and 50m, respectively (the net distance after removing the vehicles' dimension). The second platoon (indicated with blue vehicles) has four CAVs moving in two rows and two columns toward left ($\theta=\pi$); with the initial lateral distance of 2m and longitudinal distance of 100m. Note that the CAVs' initial configurations and physical parameters are identical.

Table 1 shows the assigned value for the parameters in this experiment. The initial speed for the CAVs is set to 27.8m/s. Since the initial relative speed for the vehicles that belong to the same platoon is zero, according to (7), the CAVs has no threats at the beginning of

simulation. However, for the vehicles from different platoons, the relative speed is not zero. Thereby, when the two platoons get closer, the CAVs begin to detect the threats. Based on (7), when the relative distance of the two platoons reaches to v_0^2/a_{dec} (roughly 84m), the two red vehicles that are heading toward the blue platoon identify the two other vehicles with the same lateral position as their threats and form two threat clusters. These two clusters will merge to one bigger cluster of four mentioned CAVs, when the diagonal distance between them get smaller than 84m. Consequently, as it is shown in Figure 5, the both CAVs' platoons change their configuration to make the required lateral free space to pass without collision. In the same manner, as it goes further with time, the CAVs from the other columns join the threat cluster (for instance time steps 110, 130, and 150), and some other CAVs that complete the action regards to collision avoidance leave the threat cluster (time steps 120, 140, 160, and 200). For instance at time step 120, the two heading vehicles of blue platoon make a threat clusters with the two vehicles in the middle of the second column. Meanwhile the red vehicles of the first column that previously belong to threat cluster are not threat anymore.

As one can observe in Figure 5, the threat clusters are dynamically changing over time. At the begining of the simulation, the number of vehicles that are involved in the threat clusters are small (4 vehicles at time steps 90 and 100). By decreasing the relative distance among the platoons and approaching the second column of blue platoon the number of CAVs engaged in threat groups increases (13 and 12 vehicles at time steps 130 and 150, respectively). At time step 160, when the first column of blue platoon completely pass, the number of threat vehicles decreases again. Utilizing the concept of threats and clusters, enables the decentralizing of the control. Instead of controlling all the vehicles and considering all the relations among them, we only controlling the vehicles that are threatened and eliminating all the unnecessary relations. As an example, at time step 140, instead of solving one optimization problem for all the 16 vehicles (an MPC with $360p$ constraints), solving two optimization problems each of them with 5 vehicles is proposed (an MPC with $67p$ constraints). Accordingly, it reduces the dimensions of optimization problem and the computational time. Note that in this experiment, the prediction horizon p is considered equal to 8. Since the clusters and optimization problem is changing frequently, setting a higher prediction horizon cannot improve the results.

Table 1: The simulation parameters values.

T	T_{cd}	w	$v_{\max}$	$a_{\max}$	$a_{\min}$	a_{dec}	α	δ	δ_a	δ_θ
0.05 s	1.2 s	2 m	33.3 m/s	5.7 m/s^2	-10.9 m/s^2	9 m/s^2	2.5 m	0.5 m	0.7 m/s^2	$\pi/30$ rad

In order to verify the collision-free movement of CAVs, we investigate the minimum net lateral distance between CAVs (resulted from the introduction of constraint (9)). During the entire simulation time, the minimum value associates with the time step 190 and is 0.96m, which is bigger than the assigned value to δ (i.e., 0.5m). In conclusion, the designed control method successfully manages the platoons movements to pass without collision.

As we explained in the control approach, beside the collision avoidance objective, the MPC controller is developed to optimize the system performance in terms of reaching the desired speed. Hence, the objective function (8) is designed to minimize the deviation of

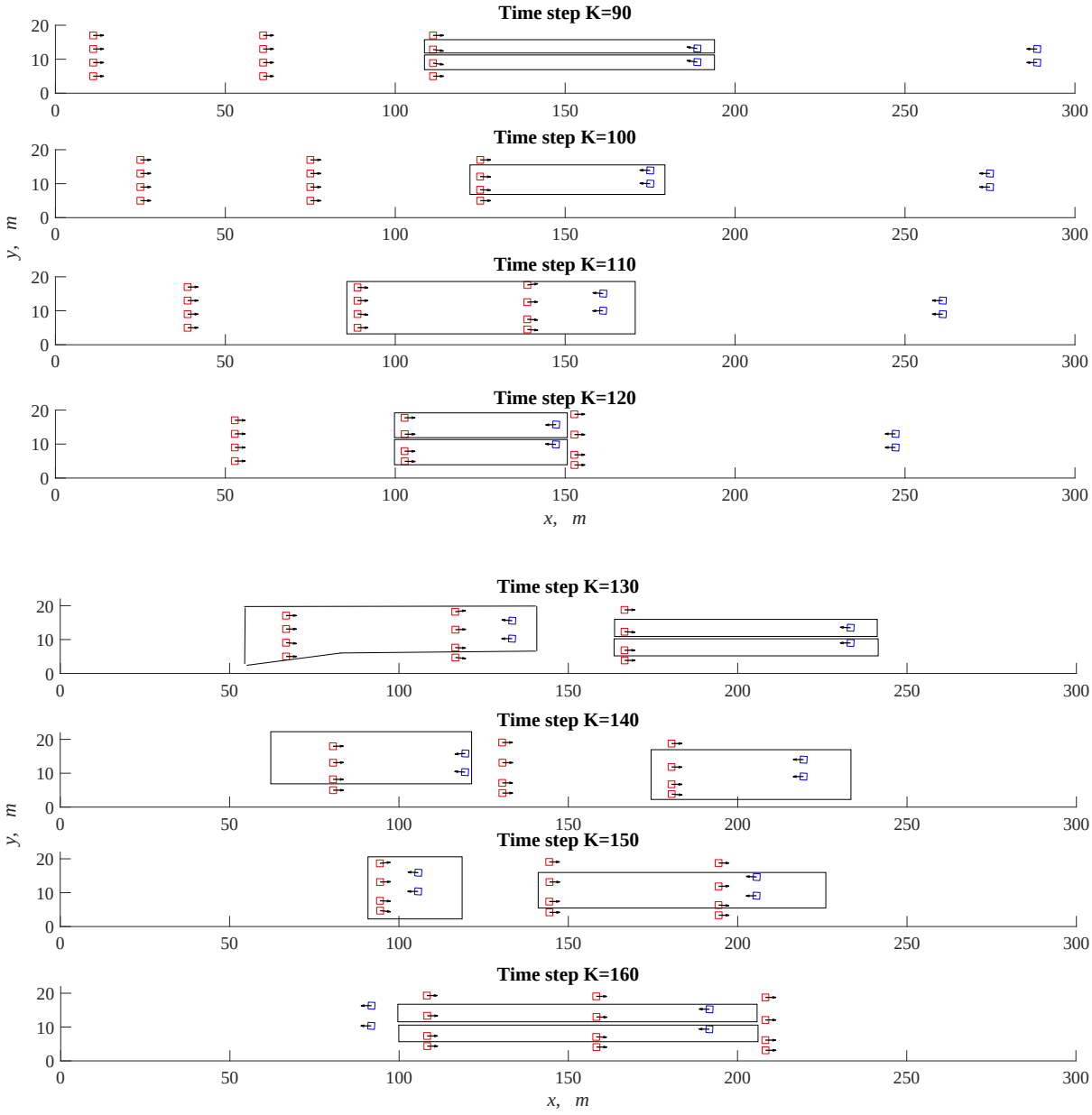

Figure 5: Displaying CAVs' positions in the highway for the simulation case study at different time steps.

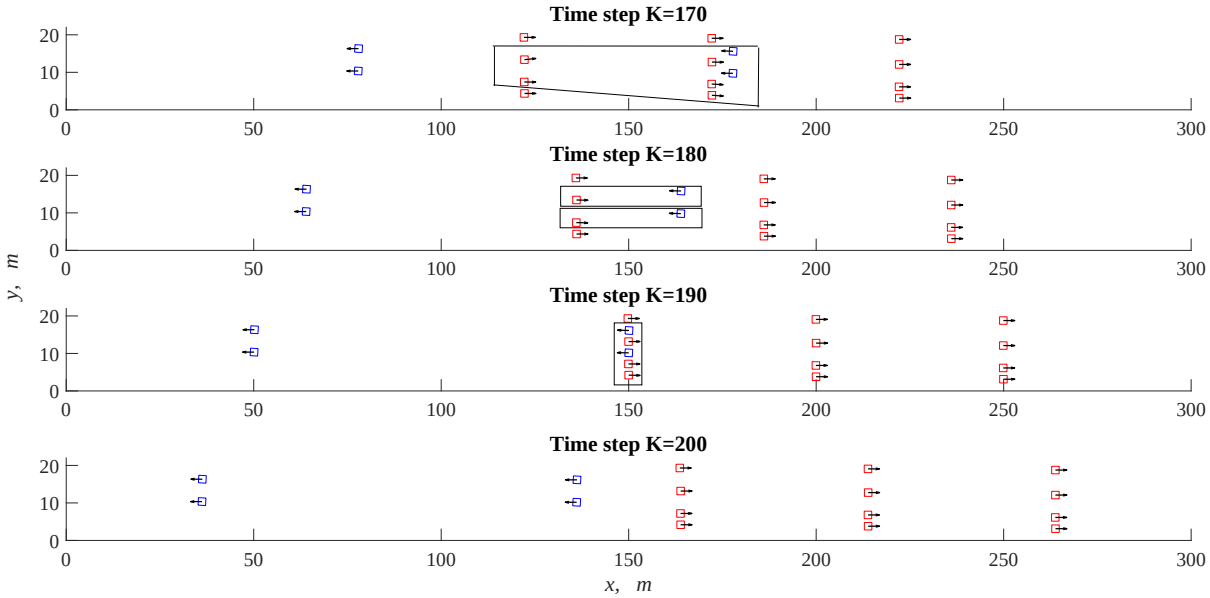

speed and heading angle from their desired values. In order to evaluate this objective, we employ the Root Mean Square Error (RMSE) concept. For variable f with the desired value of f^d the RMSE error is calculated as follows.

$$\text{RMSE} = \sqrt{\frac{1}{N}\sum_{i=1}^{N}(f(i) - f^d)^2} \tag{16}$$

Thanks to (16) we calculate the RMSE error for the speed v, the acceleration a and the heading angle θ for all the CAVs involved in this case study, over the time step interval of $[90 - 190]$. The RMSE error for the speed and the heading angle are $0.0146\,\text{m/s}$, $0.1619\,\text{m/s}^2$, and 0.0338 rad, respectively. The very small value of RMSE error for the speed indicates that although in this experiment, we had two contradicting platoons of CAVs moving toward each other with high speed, the CAVs could always move with their desired speed. In other words, the proposed methodology can improve the travel time for CAVs. In addition, the small value of RMSE error for the control signals, θ and a, show the low energy cost and the optimality of the performance.

5 Conclusion and Future Work

In this paper, we have introduced the concept of laneless and directionless movement as a new possibility for CAVs behavior in motorway networks. To represent the relations between CAVs in this environment, we presented the notions of neighborhood, threat, and threat group. Thanks to these three relation-based notions, we developed a decentralized control strategy for CAVs movement based on MPC. The control objective is defined so as to avoid collision and meanwhile retain the optimality in traffic performance. Finally, the functionality of the proposed method is investigated with a simulation experiment. The simulation of the case study demonstrates promising results, which motivates the further research and applications. For the future work, we aim at simulating various traffic flow phenomena and characteristics of CAVs traffic on a highway, and compare the results with the merely laneless strategy to show the advantages of adding the directionless freedom.

6 References

Asaithambi, G., V. Kanagaraj and T. Toledo (2016) Driving behaviors: Models and challenges for non-lane based mixed traffic, *Transportation in Developing Economies*, **2** (2) 1–16.

Chavan, R., A. K. Mulla, D. Chakraborty and D. Manjunath (2016) A model for lane-less traffic with local control laws, paper presented at the *Proceeding of the 2016 European Control Conference (ECC)*, 2447–2452, Aalborg, Denmark, June 29-July 1.

Chavoshi, K., A. Genser and A. Kouvelas (2021) A pairing algorithm for conflict-free crossings of automated vehicles at lightless intersections, *Electronics*, **10** (14), ISSN 2079-9292.

Chavoshi, K. and A. Kouvelas (2020) Cooperative distributed control for lane-less and direction-less movement of autonomous vehicles on highway networks, paper presented at the *9th Symposium of the European Association for Research in Transportation (hEART 2020)*.

Elliott, D., W. Keen and L. Miao (2019) Recent advances in connected and automated vehicles, *J. Traffic and Transportation Engin.*, **6** (2) 109–131.

Gueriau, M., R. Billot, N. E. Faouzi, J. Monteil, F. Armetta and S. Hassas (2016) How to assess the benefits of connected vehicles? a simulation framework for the design of cooperative management strategies, *Transportation Research Part C: Emerging Technologies*, **67**, 266–279.

Hancock, P. A., I. Nourbakhsh and J. Stewart (2019) On the future of transportation in an era of automated and autonomous vehicles, *Proceedings of the National Academy of Sciences*, **116** (16) 7684–7691.

He, Z., L. Zheng, L. Lu and W. Guan (2018) Erasing lane changes from roads: A design of future road intersections, *IEEE Transactions on Intelligent Vehicles*, **3** (2) 173–184.

Kim, K.-D. and P. R. Kumar (2014) An mpc-based approach to provable system-wide safety and liveness of autonomous ground traffic, *IEEE Transactions On Automatic Control*, **59** (1) 3341–3356.

Makarem, L. and D. Gillet (2013) Model predictive coordination of autonomous vehicles crossing intersections, paper presented at the *Proceeding of the 16th International IEEE Annual conference on intelligent Transportation Systems (ITSC 2013)*, 1799–1804, Hauge, Netherlands, October 6-9.

Malekzadeh, M., I. Papamichail and M. Papageorgiou (2021) Internal boundary control of lane-free automated vehicle traffic using a model-free adaptive controller, *IFAC-PapersOnLine*, **54** (2) 99–106, ISSN 2405-8963. 16th IFAC Symposium on Control in Transportation Systems CTS 2021.

Mitrovic, N., I. Dakic and A. Stevanovic (2019) Combined alternate-direction lane assignment and reservation-based intersection control, *IEEE Transactions on Intelligent Transportation Systems*.

Mulla, A. K., A. Joshi, R. Chavan, D. Chakraborty and D. Manjunath (2019) A microscopic model for lane-less traffic, *IEEE Transactions on Control of Network Systems*, **6** (1) 415–428.

Nguyen, L. X., S. Hanaoka and T. Kawasaki (2014) Traffic cponflict assumption for non-lane-based movements of motorcycles under congested conditions, *International Association of Traffic and safety Science Research*, **37**, 137–147.

Papageorgiou, M., K.-S. Mountakis, I. Karafyllis, I. Papamichail and Y. Wang (2021)

Lane-free artificial-fluid concept for vehicular traffic, *Proceedings of the IEEE*, **109** (2) 114–121.

Talebpour, A., H. S. Mahmassani and A. Elfar (2017) Invastigating the effects of reserved lane for autonomous vehicles on congestion and travel time reliability, *Transportation Research Record: Journal of the Transportation Research Board*, **2622** (1) 1–12.

Talebpour, A., H. S. Mahmassani and S. H. Hamdar (2015) Modeling lane-changing behavior in a connected environment: A game theory approach, *Transportation Research Procedia*, **7**, 420–440.

Troullinos, D., G. Chalkiadakis, I. Papamichail and M. Papageorgiou (2021a) Collaborative multiagent decision making for lane-free autonomous driving.

Troullinos, D., G. Chalkiadakis, I. Papamichail and M. Papageorgiou (2021b) *Collaborative Multiagent Decision Making for Lane-Free Autonomous Driving*, 1335–1343, International Foundation for Autonomous Agents and Multiagent Systems, Richland, SC, ISBN 9781450383073.

Wang, Z., Y. Bian, S. E. Shladover, G. Wu, S. E. Li and M. J. Barth (2019) A survey on cooperative longitudinal motion control of multiple connected and automated vehicles, *IEEE Intelligent Transportation Systems Magazine*, **12** (1) 4–24.

Xu, B., S. E. Li, Y. Bian, S. Li, X. J. Ban, J. Wang and K. Lia (2018) Distributed conflict-free cooperation for multiple connected vehicles at unsignalized intersections, *Transportation Research Part c: Emerging Technologies*, **93**, 322–334.

Zheng, Z. (2014) Recent developments and research needs in modeling lane changing, *Transportation research part B: methodological*, **60**, 16–32.

Zhou, M., X. Qu and S. Jin (2017) On the impact of cooperative autonomous vehicles in improving freeway merging: A modified driver model-based approach, *IEEE Transactions On Intelligent Transportation Systems*, **18**, 1422–1428.

Zhu, W. nd H. M. Zhang (2018) Analysis of mixed traffic flow with human-driving and autonomous cars based on car-following model, *Physica A: Statistical Mechanics and its Applications*, **496**, 274–285.